Review of Scientific Instruments

Foucault pendulum properties of spherical oscillators

Cite as: Rev. Sci. Instrum. **91**, 095115 (2020); https://doi.org/10.1063/5.0010759
Submitted: 30 April 2020 . Accepted: 07 September 2020 . Published Online: 23 September 2020

P. Flückiger, I. Vardi, and S. Henein

View Online Export Citation CrossMark

ARTICLES YOU MAY BE INTERESTED IN

Time-scaling vibrato musical tones while retaining vibrato rates
Proceedings of Meetings on Acoustics **31**, 035005 (2017); https://doi.org/10.1121/2.0001297

Real-time tracking of protein unfolding with time-resolved x-ray solution scattering
Structural Dynamics **7**, 054702 (2020); https://doi.org/10.1063/4.0000013

Train Noises and Use of Adjacent Land
Sound: Its uses and Control **1**, 10 (1962); https://doi.org/10.1121/1.2369546

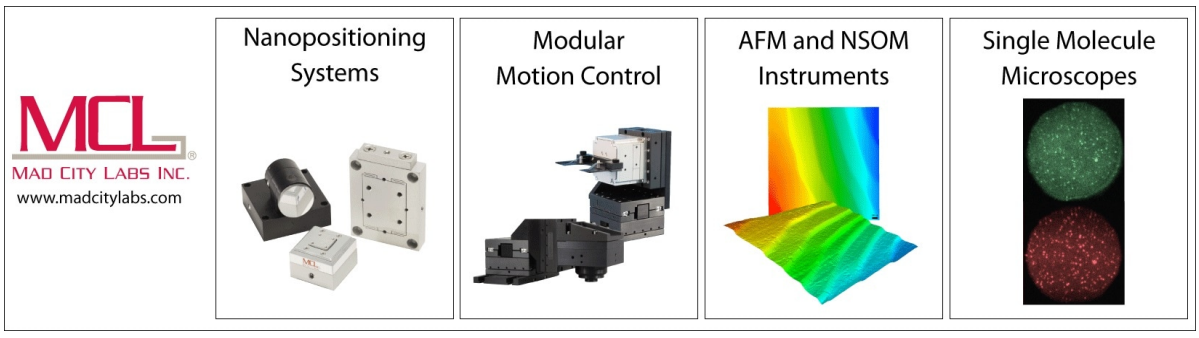

© 2020 Author(s).

Review of Scientific Instruments ARTICLE scitation.org/journal/rsi

Foucault pendulum properties of spherical oscillators

Cite as: Rev. Sci. Instrum. 91, 095115 (2020); doi: 10.1063/5.0010759
Submitted: 30 April 2020 • Accepted: 7 September 2020 •
Published Online: 23 September 2020

View Online Export Citation CrossMark

P. Flückiger,[a] I. Vardi,[b] and S. Henein[c]

AFFILIATIONS

EPFL, Instant Lab, Rue de la Maladiere 71b, 2000 Neuchatel, Switzerland

[a]Author to whom correspondence should be addressed: patrick.fluckiger@epfl.ch
[b]ilan.vardi@epfl.ch
[c]simon.henein@epfl.ch

ABSTRACT

The Foucault pendulum provides a demonstration of the turning of the Earth. The principle at work is that linear oscillations of a two-degree-of-freedom isotropic harmonic oscillator remain unchanged in an inertial frame of reference, so appear to precess in a rotating frame of reference. In recent work, we applied two-degree-of-freedom isotropic oscillators to mechanical timekeeping. In this paper, we note that the spherical oscillators we considered have qualitatively different behavior in a non-inertial frame. We show that when in a rotating frame, linear oscillations precess at one half the rotational speed of the rotating frame. We validate this result experimentally by designing and constructing a proof of concept demonstrator placed on a motorized rotating table. The demonstrator consists of a spherical isotropic oscillator, a launcher to place the oscillator on planar orbits, a motorized rotating table, video recording for qualitative observation, and a laser measurement setup for quantitative results. The experimental data recorded by the lasers strongly validate the physical phenomenon.

© 2020 Author(s). All article content, except where otherwise noted, is licensed under a Creative Commons Attribution (CC BY) license (http://creativecommons.org/licenses/by/4.0/). https://doi.org/10.1063/5.0010759

I. INTRODUCTION AND STATEMENT OF RESULTS

A. The Foucault pendulum

In 1851, Léon Foucault created a sensation with his pendulum providing a direct demonstration of the turning of the Earth; for a historical description, see Refs. 4 and 15. This simple device consists of a spherical pendulum whose mass is launched in a purely linear orbit. Following Mach's principle of inertia, the mass will continue to oscillate in the same linear orbit with respect to absolute space. For an observer on the Earth, however, the plane of oscillation will precess. Conceptually speaking, Foucault constructed a very precise demonstrator showing that, when put on a rotating table, linear oscillations of a harmonic isotropic two-degree-of-freedom (2-DOF) oscillator, see below, remain linear with respect to an inertial frame of reference. Indeed, the standard proof of the Foucault phenomenon (see Ref. 2, Chap. 4) assumes that the vertical motion of the pendulum and its isochronism defect are negligible and prove the result for a harmonic 2-DOF oscillator.

B. 2-DOF oscillators and their application to mechanical timekeeping

Recently, our EPFL laboratory has considered harmonic isotropic 2-DOF oscillators applied as time bases for mechanical timekeepers, with results communicated in a series of papers.[12,16] The advantage of using these time bases is that they no longer need the complex escapement mechanism required in all previous mechanical timekeepers. The specifications for such harmonic isotropic 2-DOF oscillators to be mechanical time bases are the following:

1. A 2-DOF oscillator.
2. A linear restoring force, i.e., obeys Hooke's law.
3. A central restoring force, i.e., the spring potential has a unique minimum.
4. The central restoring force is *isotropic,* i.e., it is the same in all radial directions.
5. The mobile mass behaves as a particle, i.e., as a point mass.
6. Mass is independent of position.
7. Motion is restricted to a plane.

© Author(s) 2020

8. Chronometric accuracy is insensitive to oscillator energy (isochronism).
9. Chronometric accuracy is insensitive to the direction of gravity.

Conditions 1–6 were already considered in 1687 by Isaac Newton in his *Principia Mathematica*, Book I, Proposition X,[10] where he showed that they imply conditions 7 and 8. Newton showed that there are unidirectional closed orbits, which are ellipses with the center of force at the center of the ellipse and period of rotation the same for all ellipses (isochronism). Our basic contribution was to note that this isochronism means that the oscillator can be used as a time base for an accurate timekeeper and that unidirectional orbits eliminate the need for a classical escapement mechanism. Note that condition 9 applies only to portable timekeepers such as watches but not to clocks.

C. Spherical oscillators

We have so far been unable to satisfy all these conditions. Our first realization satisfied conditions 1–8 but not condition 9 and was realized in a clock.[12] In order to satisfy condition 9, we considered *spherical oscillators,* since the sphere is symmetric and relatively insensitive to the direction of gravity. However, spherical oscillators violate condition 7 and it follows that isochronism no longer holds. In our previous paper,[16] we chose a central restoring force we called the *Scissors Law* (see Sec. II D), and for which all circular orbits have the same period, what we call *circular isochronism.* This spherical oscillator was also realized as a time base for the clock shown in Fig. 1.[9] This fully functional clock was exhibited at the International Museum of Horology, La Chaux-de-Fonds, Switzerland, in September 2017.[8]

FIG. 1. Mechanical clock without escapement using a spherical oscillator time base. Reprinted with permission from Ref. 9, Instant-lab 2016 Annual Report, downloadable at https://www.epfl.ch/labs/instantlab/page-124523-en-html/, retrieved, July 3, 2020.

Unidirectional trajectories allow the time base to bypass the escapement mechanism so that the clockwork no longer has intermittent motion characteristic of all previous mechanical timekeepers.

D. Main result: Foucault properties of spherical oscillators

In this paper, we instead examine the linear oscillations of 2-DOF oscillators. [By "linear oscillation," we mean substantially 1-DOF oscillations in which the particle passes through the center of force. Note that for a spherical pendulum, the particle trajectory lies in a single vertical plane, so these oscillations could also be called "planar".]

Since the standard proofs of the Foucault phenomenon of the spherical pendulum assume that it is actually a harmonic 2-DOF oscillator satisfying conditions 1–7, it follows that our realizations satisfying these conditions as given in Ref. 12 should also have linear oscillations exhibiting the Foucault phenomenon. However, the case of spherical oscillators was not resolved.

In this paper, we show that linear oscillations of spherical oscillators have a hybrid Foucault precession in which the line of oscillation *precesses at half the rate* of underlying rotation. The proof of this result builds on the theory developed in our previous work[16] with the further condition that the spherical oscillator is in a rotating frame (see Sec. II C). In order to validate this theory, we constructed a spherical oscillator using our previous design of Ref. 16 since this construction had already been thoroughly tested. We note that our theoretical computation shows that our main result should hold for a spherical oscillator with *any* central isotropic restoring force. We then constructed a test bench consisting of the spherical oscillator placed on a turntable with a dedicated launching mechanism to ensure linear oscillations and lasers to provide accurate data of the oscillation direction (see Sec. IV). We also placed a camera to film the oscillations in order to provide visual confirmation of the phenomenon.

II. THEORY

A. Kinematics

The first specification we address is condition 1, which requires restricting motion to two degrees-of-freedom. We do this by having our spherical mechanisms obey *Listing's law,* which is a restriction on spherical rotation reducing the number of degrees-of-freedom of rotation from three to two. These kinematics were introduced by Johannes Benedict Listing (1808–1882) and subsequently named *Listing's law* by Helmholtz in Volume III of his treatise of physiological optics.[7] Its historical importance rests on the fact that it faithfully describes the kinematics of the human eye.[16]

Listing's Law. There is a direction called the *primary position* so that any *admissible* position is obtained from this position by a rotation whose axis is perpendicular to the direction of the primary position.

It follows that all axes of rotation lie on a single plane which we call the *Listing plane.* We note that Listing's law is forced by

© Author(s) 2020

specifications 1, 3, and 4 of Sec. I B since the restoring force is central and isotropic.

We follow the notation conventions of our previous paper.[16] We assume that the sphere radius equals 1. We let the primary position be such that the line of sight points to the positive x-axis. We will denote the point $\mathbf{i} = (1, 0, 0)$ as the primary position since there is only one admissible rotation with that line of sight. With these coordinates, the y–z-plane becomes the *Listing plane* containing all admissible rotational axes. Any such rotational axis can be taken to be the z-axis rotated around the x-axis by an angle φ, so represented by the unit vector $\mathbf{n} = (0, -\sin\varphi, \cos\varphi)$. One then rotates around $\mathbf{n}$ by an angle θ taking the front pole $\mathbf{i}$ to the point $\mathbf{v} = (\cos\theta, \sin\theta\cos\varphi, \sin\theta\sin\varphi)$, the $\mathbf{v}$ direction thus becomes the current line of sight. This expresses the fact that any admissible Listing position is described by the spherical coordinates (θ, φ) corresponding to the Euclidean coordinates $(\cos\theta, \sin\theta\cos\varphi, \sin\theta\sin\varphi)$ of the resulting line of sight $\mathbf{v}$, as calculated above.

We use the notation $\mathbf{R}(\alpha, \mathbf{a})$ to denote a rotation by angle α around the axis $\mathbf{a}$. The rotation $\mathbf{R}(\alpha, \mathbf{a})$ is applied to vectors on the right, so vector $\mathbf{u}$ is rotated by $\mathbf{R}(\alpha, \mathbf{a})$ to obtain vector $\mathbf{v}$ according to $\mathbf{v} = \mathbf{u}\,\mathbf{R}(\alpha, \mathbf{a})$.

B. Dynamics

As in our paper,[16] the dynamics of Listing's law is analyzed using the Euler angle formulation of rigid body rotation (see Ref. 6, p. 150 and Ref. 17, p. 9). Using the notation of Sec. II A, any rotation of a rigid body is expressed by three angles φ, θ, ψ as a rotation of angle φ around $\mathbf{i}$ taking the z-axis vector $\mathbf{k}$ to $\mathbf{n}$, followed by a rotation of angle θ around $\mathbf{n}$ taking $\mathbf{i}$ to $\mathbf{v}$, followed by a rotation of angle ψ around $\mathbf{v}$. In terms of our notation, this is the product $\mathbf{R}(\varphi, \mathbf{i})\,\mathbf{R}(\theta, \mathbf{n})\,\mathbf{R}(\psi, \mathbf{v})$.

It is seen that any Listing position (θ, φ) is obtained by the Euler angles φ, θ, $-\varphi$, that is, $\psi = -\varphi$. Using our notation, any admissible Listing rotation is the composition of rotations,

$$\mathbf{R}(\varphi, \mathbf{i})\,\mathbf{R}(\theta, \mathbf{n})\,\mathbf{R}(-\varphi, \mathbf{v}).$$

This provides an explicit formula for the angular velocity ω of a rotating body (Ref. 6, Appendix A) [Ref. 14, Eq. (10.97), p. 402]. Due to the additivity of infinitesimal rotations, the composition of rotations given by $\mathbf{R}(\varphi, \mathbf{i})$, $\mathbf{R}(\theta, \mathbf{n})\,\mathbf{R}(\psi, \mathbf{v})$ is simply derived term by term to give

$$\boldsymbol{\omega} = \dot\varphi\mathbf{i} + \dot\theta\mathbf{n} + \dot\psi\mathbf{v}.$$

Our case is $\psi = -\varphi$, so the angular velocity of admissible Listing rotations is given by

$$\boldsymbol{\omega} = \dot\varphi(\mathbf{i} - \mathbf{v}) + \dot\theta\mathbf{n}.$$

In order to set up the Lagrangian formulation of the dynamics, one computes the kinetic energy of the system. We assume that the mass density is spherically symmetric so the moment of inertia of the mass is given by the single scalar I. As shown in Ref. 16, the kinetic energy is then

$$K = \frac{I}{2}\left(\dot\theta^2 + 4\sin^2(\theta/2)\dot\varphi^2\right).$$

Given a potential $V(\theta, \varphi)$, the Lagrangian is

$$\mathcal{L} = K - V = \frac{I}{2}\left(\dot\theta^2 + 4\sin^2(\theta/2)\,\dot\varphi^2\right) - V(\theta, \varphi).$$

We restrict ourselves to *central isotropic potentials* by which we mean that potentials $V(\theta)$ do not depend on φ.

C. Foucault effect

We continue the analysis of Sec. II B, but now with the sphere rotating around its polar axis $\mathbf{i}$ at constant angular speed ζ with the angle φ now considered as a body coordinate. Due to the additivity of infinitesimal rotations, the angular velocity is now

$$\boldsymbol{\omega} = \dot\varphi(\mathbf{i} - \mathbf{v}) + \dot\theta\mathbf{n} + \zeta\mathbf{i}$$

so that

$$\|\boldsymbol{\omega}\|^2 = \dot\varphi^2\|\mathbf{i} - \mathbf{v}\|^2 + \dot\theta^2 + \zeta^2 + 2\zeta\dot\varphi - 2\zeta\dot\varphi\,\mathbf{i}\cdot\mathbf{v}.$$

Appealing to the computation of Sec. II B and $\mathbf{i}\cdot\mathbf{v} = \cos\theta$, this gives

$$\|\boldsymbol{\omega}\|^2 = \dot\theta^2 + 4\dot\varphi^2\sin^2(\theta/2) + \zeta^2 + 2\zeta\dot\varphi(1 - \cos\theta).$$

Since $1 - \cos\theta = 2\sin^2(\theta/2)$, this is

$$\|\boldsymbol{\omega}\|^2 = \dot\theta^2 + 4\dot\varphi^2\sin^2(\theta/2) + 4\zeta\dot\varphi\sin^2(\theta/2) + \zeta^2.$$

The kinetic energy is now

$$K_f = \frac{I}{2}\left[\dot\theta^2 + 4\dot\varphi^2\sin^2(\theta/2) + 4\zeta\dot\varphi\sin^2(\theta/2) + \zeta^2\right],$$

and the Lagrangian is

$$\begin{aligned}\mathcal{L}_f &= K_f - V(\theta)\\ &= \frac{I}{2}\left[\dot\theta^2 + 4\dot\varphi^2\sin^2(\theta/2) + 4\zeta\dot\varphi\sin^2(\theta/2) + \zeta^2\right] - V(\theta).\end{aligned}$$

The Euler–Lagrange equation in φ is

$$\frac{d}{dt}\left(\frac{\partial\mathcal{L}}{\partial\dot\varphi}\right) = \frac{\partial\mathcal{L}}{\partial\varphi}.$$

The right hand side is zero, since $\mathcal{L}$ does not contain any φ terms, so $\partial\mathcal{L}/\partial\varphi = 0$, so there is a constant C such that

$$\frac{I}{2}\left[8\dot\varphi\sin^2(\theta/2) + 4\zeta\sin^2(\theta/2)\right] = C.$$

This simplifies to

$$(2\dot\varphi + \zeta)\sin^2(\theta/2) = D$$

for a constant D.

The key observation is that this equation can be satisfied when $\dot\varphi = -\zeta/2$. This means that there are solutions consisting of linear trajectories precessing at a rate one half of the constant sphere rotation. This is exactly our main theoretical result.

D. Scissors law

Our main result holds for any central isotropic potential, but in order to construct a physical model, we must make a particular choice. We decided on keeping the same potential as in our previous paper[16] since this would allow us to use the design established in that paper.

In our previous paper,[16] we noted that spherical oscillators do not follow the specifications of Sec. I, so isochronism of arbitrary orbits is no longer possible. Since isochronism is the fundamental property for precise timekeeping, we considered a weaker form

© Author(s) 2020

Definition. Circular isochronism means that circular steady state orbits all have the same period.

In Ref. 16, we showed that the potential

$$V_s = \kappa \sin^2(\theta/2), \text{with constant } \kappa \tag{1}$$

leads to circular isochronism. We called this the *Scissors Law* since its mechanical realization resembles scissors. Since this is a central isotropic potential, our main result on Foucault precession holds.

The Euler–Lagrange equation in θ is

$$\frac{d}{dt}\left(\frac{\partial \mathcal{L}}{\partial \dot{\theta}}\right) = \frac{\partial \mathcal{L}}{\partial \theta},$$

which gives

$$I\ddot{\theta} = I\dot{\varphi}^2 \sin\theta + I\zeta\dot{\varphi}\sin\theta - V_s'(\theta),$$

where

$$V_s'(\theta) = \frac{dV_s}{d\theta} = \frac{\sin\theta}{2},$$

which gives the equation

$$\ddot{\theta} - \left(\dot{\varphi}^2 + \zeta\dot{\varphi}\right)\sin\theta + \frac{\kappa}{2I}\sin\theta = 0.$$

Note that when $\zeta = 0$ and $\dot{\varphi} = 0$, the mechanism has purely planar oscillation satisfying

$$\ddot{\theta} + \frac{\kappa}{2I}\sin\theta = 0.$$

This is just the equation of a simple pendulum, so the scissor sphere oscillator has the same dynamics as the simple pendulum for purely linear oscillations. As is well known for small θ, one can apply the approximation $\sin\theta \approx \theta$ to get the equation

$$\ddot{\theta} + \frac{\kappa}{2I}\theta = 0,$$

which approximates the dynamics as the amplitude approaches zero. The *nominal frequency* of purely linear oscillations is therefore

$$\frac{1}{2\pi}\sqrt{\frac{\kappa}{2I}}.$$

In our situation of constant rotation ζ and Foucault precession $\dot{\varphi} = -\zeta/2$, the equation in θ becomes

$$\ddot{\theta} + \left(\frac{\kappa}{2I} + \frac{\zeta^2}{4}\right)\sin\theta = 0.$$

It follows that the nominal frequency increases from

$$\frac{1}{2\pi}\sqrt{\frac{\kappa}{2I}}$$

to

$$\frac{1}{2\pi}\sqrt{\frac{\kappa}{2I} + \frac{\zeta^2}{4}}.$$

This means that polar rotation leads to an effective increase in the stiffness of the scissor spring.

Remark. This increase in stiffness is contrary to what one would expect with a rotating pendulum, as the centripetal force would cancel the gravitational restoring force, so frequency should decrease in that case.

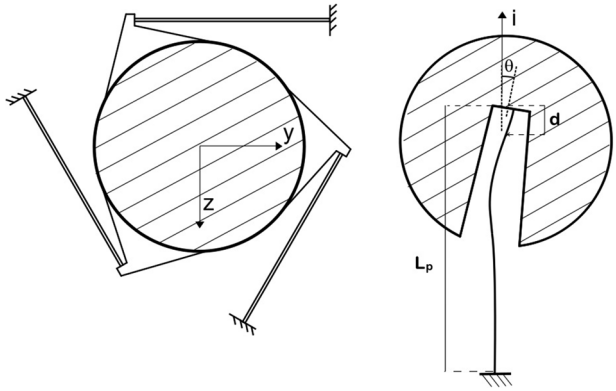

FIG. 2. Schematic design depicting the three equatorial beams (left) and the polar beam (right).

III. DESIGN

A. Description of the design

Our design is based on the oscillator time base of our previous paper.[16] This design realizes Listing's law, acts as a suspension, as the mechanism operates under a gravitational field, and the central isotropic restoring force was chosen to obey the Scissors Law.

In analogy with a terrestrial globe if we consider the line of sight as the north pole, we showed in Ref. 16 that three identical equally distributed equatorial linear springs produce a scissors law restoring torque acting toward the principal position and restricting the kinematics to Listing's law. In addition, a single polar beam is added to provide an adequate suspension for the mechanism. Following a well-known result of Wittrick,[18] we suspend the sphere on the polar beam above the center of the sphere at a ratio of 1/8 above center and 7/8 below center in order to minimize the parasitic shift of the center in the x direction, so $d = L_p/8$ in Fig. 2. The three equatorial beams are arranged by a 120° consecutive rotation about the center O in the equatorial plane (y- z-plane, see Fig. 2).

Since our model only uses three equatorial springs and one spring as a suspension, it appears to be the simplest possible realization of a spherical oscillator obeying Listing's law and approximating a scissors law.

IV. CONSTRUCTION AND EXPERIMENTAL DATA

A. General design, specs, and dimensions

The goal being to study the behavior of the spherical oscillators with strictly linear oscillations when placed in a vertically rotating frame, the demonstrator therefore consists in an oscillator, a measurement system, a device capable of putting the oscillator into rotation, and a system to launch it on linear orbits.

The design of the oscillator was based on the previously built clock oscillator. Indeed, there are three equatorial beams and a polar beam. One important difference with the clock is that in this application, the polar beam is placed beneath the spherical mass to increase the visibility of the sphere (for its demonstrator purpose), and this beam, therefore, works in compression. The oscillating mass is based

© Author(s) 2020

on a steel hollow sphere with an outer diameter of 170 mm and a thickness of 8.3 mm, giving a theoretical mass and moment of inertia of 5.3 kg and 2.3×10^{-2} kg m^2, respectively. The additional parts (screws, pins) and actual construction result in a mass and moment of inertia of 5.32 kg and 2.05×10^{-2} kg m^2, respectively. The equatorial beams are made from spring steel with a square cross section of 1×1 mm^2 and a length of 161 mm. The polar beam is also out of spring steel with a circular cross section of 2 mm in diameter for a length of 210 mm.

Using a previously established analytical model, the considered spherical mass and beams lead to an oscillator with a theoretical frequency of 1.75 Hz.

The design following that of the clock, the three equatorial beams are, in fact, a single sheet of steel, which is clamped by two aluminum parts that form what we will define as the *equatorial ring* (see Fig. 3). We take advantage of this equatorial ring in the implementation of the measurement system. The setup consists of a pair of distance-measuring lasers that target the equatorial ring at two locations from above. Indeed, as the oscillator has two degrees-of-freedom, two lasers are necessary and sufficient in determining the orientation of the sphere (Figs. 4 and 5).

Putting the oscillator in a rotating frame is necessary for the Foucault effect to be seen with the naked eye (the Foucault effect due to the Earth's rotation being extremely small) and to increase the Foucault phenomenon with respect to the parasitic effects of the oscillator. In order to achieve this, the oscillator is placed on a turntable, which simply consists in a motorized rotation stage for optical experiments (Standa motorized Rotary Stage 8MR191-28).

A launching system of the oscillator is needed. Indeed, when the turntable is put into rotation, there is an acceleration phase before reaching a constant angular velocity. If the oscillator is already on planar orbits before putting the turntable into rotation, the acceleration phase could disturb its behavior. The launching system will therefore keep the oscillator tilted during the acceleration of the turntable, then release it. To release the sphere with no initial velocity, a simple method is to maintain the sphere tilted with a latch that will be removed (via a controlled solenoid). Moreover, the launching direction was to be adjustable as to allow the launching direction to be modified. Here, again, the equatorial ring is used to our advantage, providing a surface all around the sphere on which the latch can press.

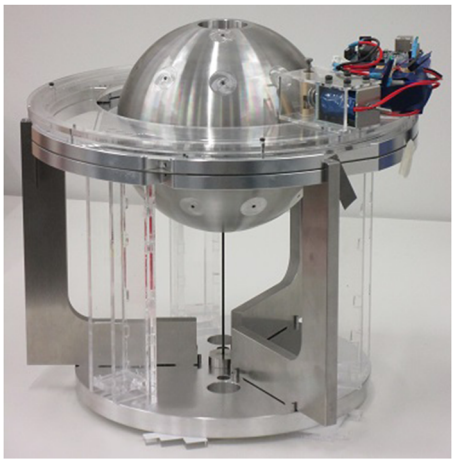

FIG. 4. Construction of the oscillator. Three additional pillars of PMMA used for the assembly can be seen.

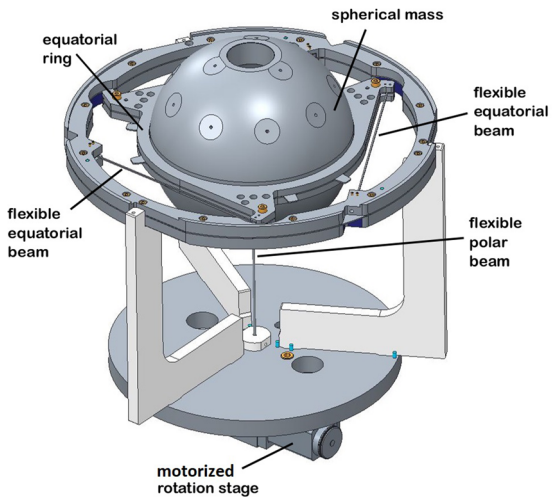

FIG. 3. CAD model of the oscillating mass with its three laser cut equatorial beams. The mass consists of two hollow hemispheres and two aluminum clamping plates. The oscillator is placed on a motorized rotating stage.

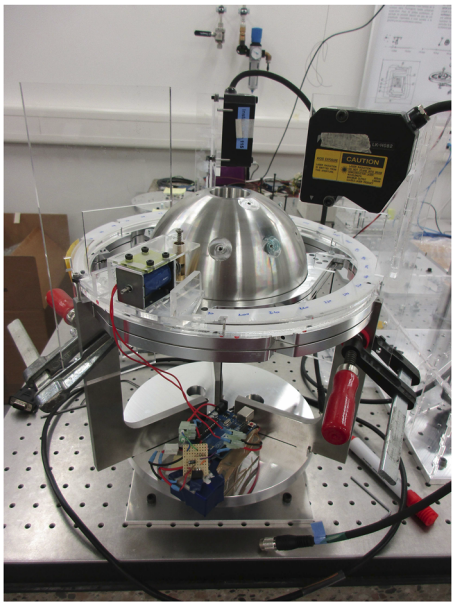

FIG. 5. Experimental setup comprising the oscillator, the motorized rotation stage, the removable latch to release the sphere, and the pair of lasers to record the position of the spherical mass.

© Author(s) 2020

B. Characterization of the oscillator

A critical aspect to consider is the anisotropy in the stiffness and inertia of the system. Indeed, as is well known, if the principal frequencies of a 2-DOF harmonic oscillator are unequal, then the elliptical orbits corresponding to Newton's model of Sec. I become *Lissajous figures* and degenerate to orbits that diverge from the roughly linear orbits. Thus, any isotropy defect, i.e., inequality between principal frequencies, can lead to degeneration of the roughly linear orbits that can exhibit Foucault precession. This effect also holds for the classical Foucault pendulum, especially for short pendulums. Minimizing isotropy defect was first addressed by 1913 Nobel laureate Heike Kamerlingh Onnes in his 1879 doctoral thesis, a topic suggested by Gustav Kirchoff (see Refs. 2, 13, and 15). A further method is the *Charron ring*, which is a simple mechanism to reduce the divergence from linear trajectories.[2,3,13] Finally, experimental and theoretical evidence indicates that maintaining the pendulum reduces the divergence from linear orbits.[11]

We have not attempted to minimize isotropy defect, and our measurements indicate that the relative difference between principal frequencies of our construction is approximately 1% (see Table I).

As shown in Fig. 6(a), for an immobile turntable, an initially linear orbit will degenerate to then return to a linear orbit symmetrically opposite the slow axis. This provides an easy method to find the principal axes. This method consists in launching the sphere in an arbitrary direction, and once the orbit becomes linear again (symmetrically to the slow axis), the direction is observed. The slow principal axis is therefore in the middle of the two previous linear orbits. One can note that if the oscillator is launched along the slow principal axis, then the orbit will not be affected by the isotropy defect and remain linear. We take advantage of this last property in the Foucault effect measurements by launching the sphere along the slow principal axis. Even though the orbit will depart from the slow principal axis, staying close to the principal axis will minimize the effect of the isotropy defect.

In the frame described by the now determined principal axes, our oscillator can be considered as two independent 1-DOF oscillators, each with their own frequency and quality factor. The oscillator was characterized by determining the position of the principal axes along with their respective frequencies and quality factors. The

TABLE I. Frequencies and quality factors for each principal axis. The isotropy defect is the relative difference between principal frequencies $(f_y - f_x)/f_x \times 100\%$. Most relevant quantities are in bold.

Parameter	Value
Time measured for 20 oscillation	11.54 (s)
Frequency along x	**1.733 (Hz)**
Slope of linear regression	−0.0125
Quality factor Q_x	**435**
Time measured for 20 oscillation	11.39 (s)
Frequency along y	**1.755 (Hz)**
Slope of linear regression	−0.0127
Quality factor Q_y	**434**
Isotropy defect	1.27%

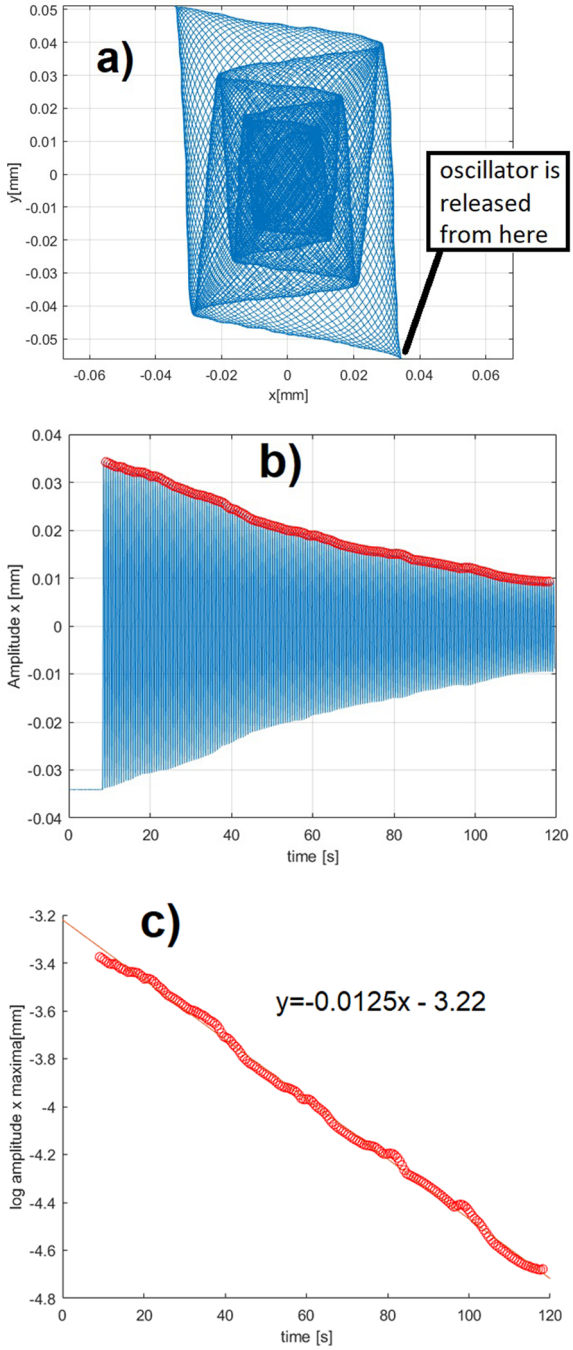

FIG. 6. Example of data used for the characterization of the oscillator. (a) Trajectory of the sphere launched on a linear orbit in an arbitrary direction for an immobile turntable. One can easily recognize a Lissajous figure with decay, the principal axes being the x and y-axes of the graph. (b) x projection of the trajectory of the sphere, with the maxima highlighted. As the trajectory was represented in the frame of the principal axes, the x component of the sphere is a damped 1-DOF oscillator. This graph enables the frequency to be calculated by measuring the time required to do 20 (arbitrarily chosen) oscillations. (c) Log of the maxima of (b) with its linear regression. The slope of the regression is inversely proportional to the quality factor Q.

© Author(s) 2020

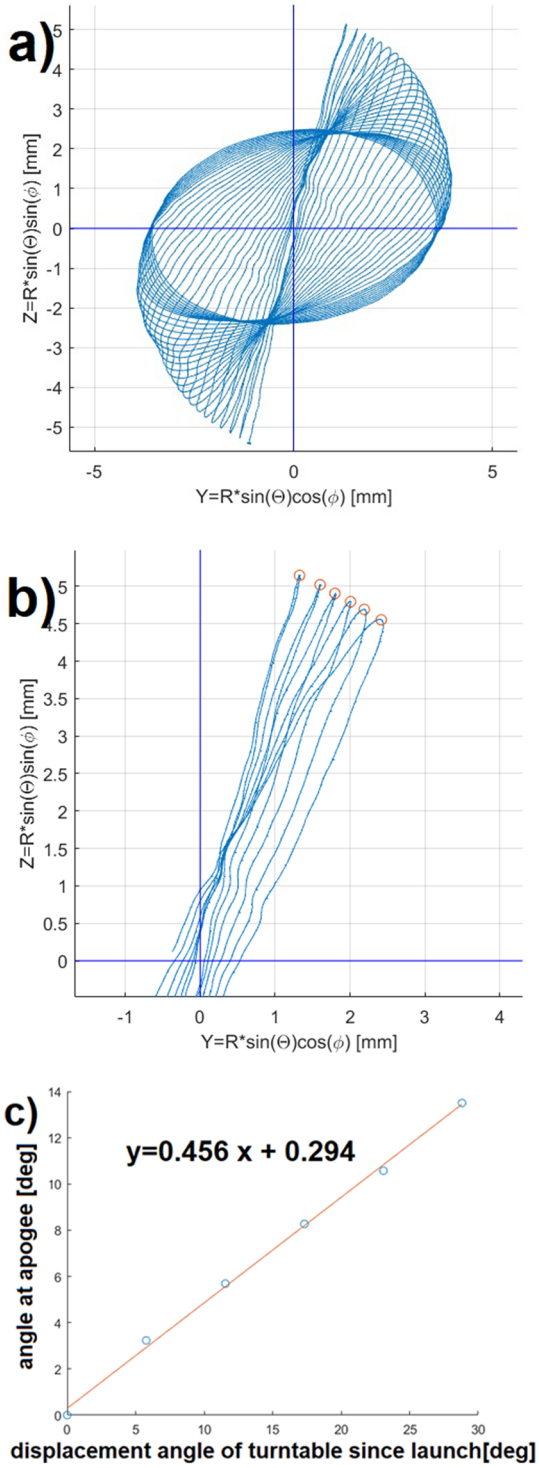

FIG. 7. Example of data used to determine the precession rate of our oscillator. (a) Position of the top of the sphere projected onto the equatorial plane for a table turning at 10°/s. (b) Enlarged view of the apogees (circles) selected for the calculations of φ. It can be seen that the orbits rapidly lose their linearity. (c) Shift angle of the plane of oscillation with respect to the shift of the table.

TABLE II. Summary of the slopes of the shift in the plane of oscillations in respect to the shift undergone by the frame.

Table speed (deg/s)	Slope of the shift in plane of oscillation vs table shift
10	0.46
6	0.57
2	0.50
1	0.51
0.5	0.75

frequency along a considered principal axis was estimated by measuring the time required to perform a certain amount of oscillations (20 oscillations were arbitrarily chosen), as shown in Fig. 6(b). The quality factors were calculated by plotting the log of the maxima [Fig. 6(c)].

The measured values and calculated frequencies and quality factors are summarized in Table I.

C. Foucault effect: Experimental method and results

Having characterized our oscillator, it was then possible to conduct the final experiments that show the Foucault phenomenon of the spherical oscillator. This involves having the turntable turn at different speeds and plotting the shift of the plane of oscillation with respect to the shift of the table. As the orbits are not perfectly linear and therefore the angle φ sweeps all possible values in a period, only the positions of the apogees were considered. Moreover, in order to limit the effect of the degradation of the initially linear orbits due to the isotropy defect, only the first six periods were considered for the measurements (as their orbits were deemed sufficiently linear). The position of each of the considered apogees was then extracted, and the evolution of the angle φ was studied. The shift angle of the apogees can be plotted with respect to time or to the table shift. According to theory, the latter should have a linear behavior with slope 1/2, which provides a simple method to validate the theory.

The sphere orientation is described by projecting the top of the sphere, the "north pole," onto the equatorial y–z-plane. An example of data is shown in Fig. 7, where Fig. 7(a) shows a full trajectory of the sphere when placed in a rotating frame, Fig. 7(b) shows the first six orbits with their apogees highlighted and Fig. 7(c) shows the angle φ with respect to the shift of the table along with the linear regression and its slope. The slopes of the linear regressions are summarized in Table II.

V. CONCLUSION AND PERSPECTIVES

This paper gives an analytical argument showing that linear orbits of 2-DOF spherical oscillators, when put in a rotating frame, precess at half the angular speed of the rotation. This phenomenon was then validated by constructing a physical model of a spherical oscillator and putting it on a turntable. The resulting data validate the analytical argument. This result is unexpected as it differs from the precession of a spherical pendulum, as first observed by Foucault in 1851, where linear orbits remain fixed in an inertial frame.

© Author(s) 2020

The natural question now is whether this phenomenon can validate the rotation of the Earth, as is the case with the classical Foucault pendulum. The first point is that our main result shows that the observed precession will have half the rotational speed of a standard Foucault pendulum, making it twice as hard to isolate. Indeed, at our latitude of 47° North, the precession will have period 64 h instead of 32 h for a Foucault pendulum.

Moreover, the Foucault phenomenon for the standard spherical pendulum is difficult to observe unless the pendulum length is quite large, well over 5 m^2, and the construction of "short pendulums," i.e., of length 1 m, is quite difficult.[5] In particular, in 1851, Airy noted that orbits that are not perfectly linear, i.e., are slightly elliptic, will precess at a rate inversely proportional to the length of the pendulum and proportional to the area of the ellipse.[1] Airy's argument applies to our realization since we showed in Sec. II D that linear orbits of our spherical oscillator have the same dynamics as the circular pendulum.

Finally, any isotropy defect will also cause unwanted precession followed by degeneration into Lissajous orbits, so a drastic reduction of the current isotropy defect of 1% (see Sec. IV B) is necessary. We are currently working on estimating the required modifications to construct a demonstrator capable of detecting the rotation of the Earth.

DATA AVAILABILITY

The data that support the findings of this study are available from the corresponding author upon reasonable request.

REFERENCES

[1]G. B. Airy, "On the Vibration of a Free Pendulum in an Oval differing little from a straight line," R. Astron. Soc. **XX**(1851), 121–130.
[2]G. L. Baker and J. Blackburn, *The Pendulum, A Case Study in Physics* (Oxford University Press, 2005).
[3]M. Charron, "Sur un perfectionnement du pendule de Foucault et sur l'entretien des oscillations," C. R. Acad. Sci. **192**, 208–210 (1931).
[4]M. F. Conlin, "The popular and scientific reception of the foucault pendulum in the united states," Isis **90**, 181–204 (1999).
[5]H. R. Crane, "Short Foucault pendulum: A way to eliminate the precession due to ellipticity," Am. J. Phys. **49**, 1004–1006 (1981).
[6]H. Goldstein, C. Poole, and J. Safko, *Classical Mechanics*, 3rd ed. (Addison-Wesley, 2000).
[7]H. von Helmholtz, in *Helmholtz's Treatise on Physiological Optics*, The Perceptions of Vision Vol. III, edited by J. P. C. Southall (Optical Society of America, 1925).
[8]Exposition temporaire—La neuchâteloise, exhibit May 6, 2017–October 8, 2017, International Museum of Horology, La Chaux-de-Fonds, Switzerland.
[9]Instant-lab 2016 Annual Report, downloadable at https://www.epfl.ch/labs/instantlab/page-124523-en-html/, Retrieved July 3, 2020.
[10]I. Newton, The Mathematical Principles of Natural Philosophy, Translated by Andrew Motte, p. 1729, Vol. 1, Google eBook, Retrieved July 3, 2020.
[11]A. B. Pippard, "The parametrically maintained Foucault pendulum and its perturbations," Proc. R. Soc. London, Ser. A **420**, 81–91 (1988).
[12]L. Rubbert, R. Bitterli, N. Ferrier, S. Fifanski, I. Vardi, and S. Henein, "Isotropic springs based on parallel flexure stages," Precis. Eng. **43**, 132–145 (2016).
[13]E. O. Schulz-DuBois, "Foucault pendulum experiment by Kamerlingh Onnes and degenerate perturbation theory," Am. J. Phys. **38**, 173–179 (1970).
[14]J. Taylor, *Classical Mechanics* (University Science Books, 2005).
[15]W. Tobin, *The Life and Science of Léon Foucault: The Man Who Proved the Earth Rotates* (Cambridge University Press, 2003).
[16]I. Vardi, L. Rubbert, R. Bitterli, N. Ferrier, M. Kahrobaiyan, B. Nussbaumer, and S. Henein, "Theory and design of spherical oscillator mechanisms," Precis. Eng. **51**, 499–513 (2018).
[17]E. T. Whittaker, *A Treatise on the Analytical Dynamics of Particles and Rigid Bodies*, 4th ed. (Cambridge University Press, 1988).
[18]W. H. Wittrick, "The properties of crossed flexure pivots, and the influence of the point at which the strips cross," Aeronaut. Q. **2**, 272–292 (1950).

© Author(s) 2020